Evaporation of Free PbS Nanoparticles: Evidence of the Kelvin Effect

K. K. Nanda,* F. E. Kruis, and H. Fissan

Department of Electrical Engineering and Information Technology, Faculty of Engineering Sciences, Gerhard-Mercator-University, 47048 Duisburg, Germany

(Received 23 August 2002; published 3 December 2002)

The size-dependent evaporation of free-spherical PbS nanoparticles has been investigated by in-flight sintering of size-classified aerosols. The temperature (T_{ev}) at which the particle size decreases due to evaporation is found to be size dependent and decreases with decreasing particle size. A linear relationship between the evaporation temperature and the inverse of the particle size is obtained as is the case with size-dependent melting of nanoparticles. This gives a direct evidence of the Kelvin effect and allows one to estimate the surface energy of nanoparticles. The surface energy of PbS nanoparticles has been found to be 2.45 $J\,m^2$.

DOI: 10.1103/PhysRevLett.89.256103 PACS numbers: 68.60.Dv, 68.35.Md

Quantum size effects, as well as the effects of large surface-to-volume ratio of nanometer-sized particles on their physical and chemical properties, have widely been explored. Apart from these two effects, the vapor pressure (p_s) of nanoparticles due to their curved surface is higher as compared to a flat surface (p_{s0}) which is given by the Kelvin equation [1]

$$\frac{p_s}{p_{s0}} = \exp\left(\frac{4\gamma M}{\rho_p RTd}\right), \tag{1}$$

where γ is the surface energy, M is the molecular weight, ρ_p is the density of the particle, R is the gas constant, T is the temperature, and d is the particle size. As a result, the vapor pressure and, hence, the evaporation of nanoparticles are predicted to be size dependent and are essential to be known for their applications at higher temperature. Recently, it has been reported [2] that the vapor pressure of the Na_{139}^+ cluster is comparable to that of bulk Na which is in contrast with the prediction of the Kelvin equation. It may also be noted that the melting temperature of the Na_{139}^+ cluster is relatively high [3]. This may be due to the higher stability of Na_{139}^+ as evident from the abundance mass spectrum [3]. Blackman *et al.* [4] have studied the evaporation of Au, Ag, and Pb nanoparticles on a carbon substrate by maintaining a constant sample temperature and found that it takes a longer time for larger particles to evaporate completely. They observed a nonlinear relation between the time of complete evaporation and particle size which is in agreement with that predicted from the Kelvin equation, although the interaction between the particle and the substrate has not been incorporated. However, one should either consider the interaction between the particle and the substrate when the experimental results are compared to the theoretical predictions or the evaporation of free particles should be investigated to eliminate the substrate effect.

In this Letter, the size-dependent evaporation of free PbS nanoparticles is investigated by on-line heat treatment of size-classified PbS aerosols at different temperatures for a particular time period. In this context, it is important to note that PbS agglomerates consisting of small particles grow into larger crystallites when sintered in the gas phase. When the sintering temperature is increased further, smaller particles are obtained due to partial evaporation [5–7]. However, PbS agglomerates deposited on amorphous carbon evaporate instead of forming larger particles when sintered [8], which implies that the influence of the substrate is significant for PbS. The temperature at which the size of the PbS particles decreases, due to evaporation (T_{ev}) under the experimental conditions used in this work, is found to decrease with decreasing particle size. Furthermore, a linear relationship has been obtained between the evaporation temperature and the inverse of the particle size as is the case with size-dependent melting [9]. This gives direct evidence of the Kelvin effect which has also been tested by condensation of vapors [10] and capillary condensation of liquids [11,12].

Details of our experimental setup can be found elsewhere [5]. In brief, a PbS aerosol is formed by sublimating PbS powder in a tube furnace and subsequent cooling down of the vapor. Nitrogen is used as a carrier gas. The aerosol is composed of agglomerates containing a number of primary particles due to Brownian coagulation of the condensation nuclei. In order to size classify the agglomerates/particles, they are charged by a radioactive β source (Kr^{85}), and flow into a differential mobility analyzer (DMA). A DMA selects particles on the basis of their mobility-equivalent diameter (D_M^{eq}), which is a function of their charge level and shape. The diameter D_M^{eq} is defined as the diameter related to the Stokes-Cunningham formula [13] and is equal to the geometric diameter for spherical and singly charged particles. After size classification, a second tube furnace enables the sintering and crystallization of the agglomerates to larger crystalline domains. The residence time of the nanoparticle aerosol in this furnace is $\sim$1.5 s when the flow of carrier gas is 1.5 slm (standard liters per minute). An

electrostatic precipitator [14] enables the aerosol to be deposited at room temperature with nearly 100% efficiency on a suitable substrate. The particle size and morphology was determined by transmission electron microscopy (TEM) (on a Philips CM12 twin microscopy, 120 keV, LaB6 cathode) and atomic force microscopy (AFM) (on a Nanoscope II, Digital instrument, Inc.).

Figure 1 shows the TEM micrographs of PbS aggregates/particles having an initial D_M^{eq} of 35 nm sintered at different temperatures. For a sintering temperature of 573 K [Fig. 1(a)], the TEM micrograph shows porous and open aggregates consisting of primary particles connected by sintering necks, whereas nearly spherical particles are obtained when the aerosol is sintered at 723 K (not shown here). This implies that the temperature of complete sintering is ~723 K for an initial D_M^{eq} of 35 nm. The main advantage of the gas-phase synthesis is the isotropic growth in all the directions which enables the growth of three-dimensional (3D) fractal aggregates and spherical quantum dots by varying the sintering temperatures. The TEM micrograph [Fig. 1(a)] for a sintering temperature of 573 K shows 2D projections of 3D fractal aggregates. Similar results have also been obtained for initial D_M^{eq} in the range 10–50 nm sintered at different temperatures. The temperature of complete sintering is found to be in between 648 and 748 K for D_M^{eq} between 10 and 50 nm. The larger the D_M^{eq}, the larger is the size of the spherical particles.

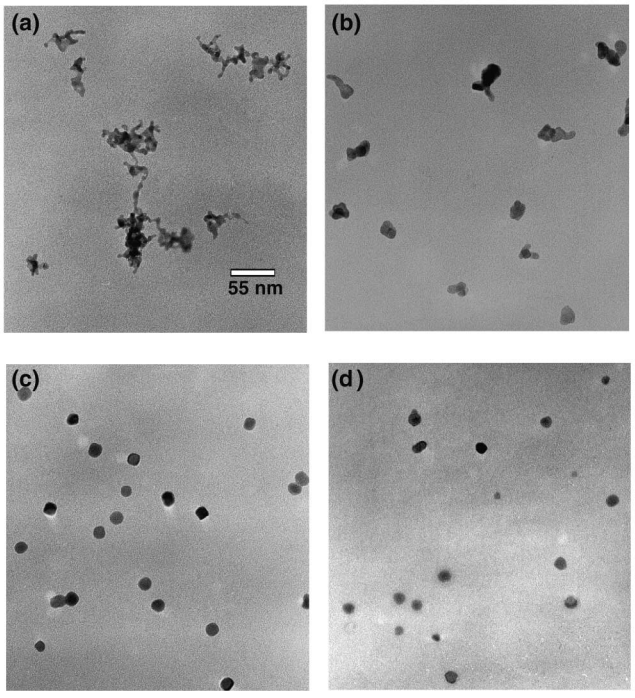

FIG. 1. TEM micrographs of PbS aggregates/nanoparticles sintered at different temperatures. The initial mobility-equivalent diameter is 35 nm. The micrographs (a)–(d) correspond to sintering temperatures of 573, 673, 748, and 773 K.

To ensure whether the sintered particles are indeed spherical, the TEM grid containing the particles sintered at 748 K having initial D_M^{eq} of 50 nm is tilted 36° (precision being better than 0.5°), with respect to the electron beam and taken the TEM micrographs. The nontilted and tilted micrographs are presented in Figs. 2(a) and 2(b) from which the dimensions of the particles as obtained from the tilted and nontilted micrographs are found to be the same (~ 21 nm). This implies that the nanoparticles are nearly spherical. The particle morphology is also studied by AFM, and the micrograph of the particles sintered at 475 °C along with the section analysis is presented in Figs. 2(c) and 2(d). Arrows in Fig. 2(d) indicate a cluster height of 20 nm (with a precision better than 0.5 nm). Figure 2(d) also indicates a lateral dimension of ~60 nm which is a consequence of the tip-object convolution effect [15]. On the basis of the agreement between the size measured by TEM and the height determined by AFM, we conclude that it is possible to obtain nearly spherical particles by in-flight sintering of the size-classified aerosol. As most of the physical processes take place in the gas phase, the shape and structure of the particles are substrate independent. Thus, this method has a distinct advantage for the synthesis of monodispersed nanoparticles of nearly spherical geometry and is advantageous, especially when the size-dependent physical properties are compared with the theoretical predictions.

The mean primary particle diameters are determined from the TEM micrographs and plotted as a function of

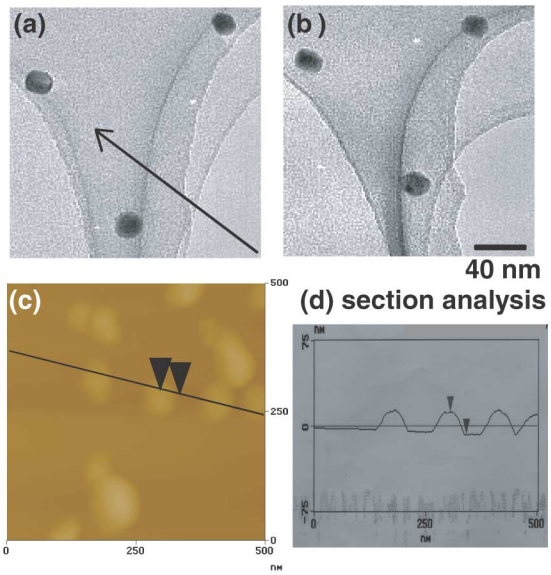

FIG. 2 (color online). TEM and AFM micrographs of PbS nanoparticles having an initial mobility-equivalent diameter of 50 nm sintered at 748 K. (a) TEM micrograph of sample normal to the electron beam, the arrow represents the axis of tilting. (b) TEM micrograph of sample tilted at 36° with respect to the electron beam; (c),(d) AFM micrograph with the section analysis.

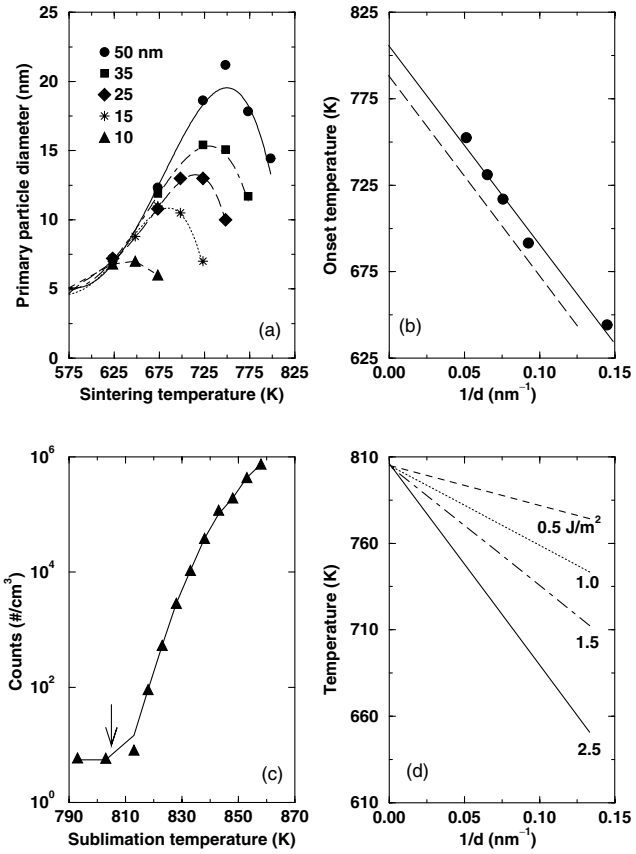

FIG. 3. (a) The diameter of the primary particles determined from the TEM micrographs as a function of sintering temperature. The initial mobility-equivalent diameter is indicated in the legend. The lines represent the fitting of each data set into a polynomial. (b) The onset temperature of evaporation is plotted against the inverse of the particle size. The solid line is a least-squares fit to the experimental data. The dashed line is an expected curve if the residence time of the aerosol in the second furnace is doubled and has been determined by estimating the decrease of the particle diameter as described in Ref. [6]. (c) The concentration of particles as a function of furnace temperature. The evaporation temperature for large particles as obtained from (b) is indicated by an arrow. (d) The size-dependent evaporation of PbS nanoparticles for different surface energy as estimated using the Kelvin equation Eq. (1).

temperature in Fig. 3(a). It can be noted that the primary particle diameter first increases and then decreases as the sintering temperature is increased. Also, the temperature of complete sintering depends on the initial D_M^{eq}. At this temperature, all the primary particles in an agglomerate merge to a single large spherical particle and the word primary particle no longer has a meaning but is used for convenience here. When the sintering temperature is increased further, the size of the nanoparticles decreases due to evaporation [5–7]. To study the size-dependent evaporation behavior of PbS nanoparticles, each set of data is fitted to a polynomial to determine the maximum particle size and the corresponding temperature which can be considered as the particle size and the onset temperature for evaporation (T_{ev}). Shown in Fig. 3(b) is the plot between the onset temperature and the inverse of the particle size, indicating that the onset temperature of evaporation is inversely proportional to the size of the nanoparticles as is the case with size-dependent melting [9]. The fitting of the experimental data into a straight line yields a slope of -1138 ± 78 nm K and an intercept of 805 ± 8 K, the latter representing the temperature where large particles start to evaporate. The evaporation temperature of large particles is very low as compared to the melting temperature (1387 K) and the boiling temperature (1554 K) of bulk PbS. Therefore, it is essential to know this temperature, especially for the synthesis of nanoparticles in the gas phase. It may be noted here that PbS sublimates from solid to vapor directly and, as a consequence, the particle evaporates at a much lower temperature as compared to the melting or boiling temperatures. As the residence time of the aerosol in the second furnace is $\sim$1.5 s, an evaporation rate of $\sim$1.0 nm/s for nanometer-sized particles is easily detectable. However, it would be difficult to detect a change of 1.0 nm in size of very large particles. If the residence time of the aerosol in the second furnace is doubled either by increasing the length of the heating zone or by reducing the flow rate, a curve as shown by the dashed line in Fig. 3(b) is expected. The dashed line has been determined by estimating the decrease of the particle diameter as described in Ref. [6]. In order to study the evaporation temperature of large particles directly, PbS powder (Aldrich Chemical Co.) with average particle size of 8 μm is sublimated in a tube furnace at different temperatures and the particle number concentration is measured using an ultrafine condensation particle counter (UCPC, TSI model 3025). The particles are formed by homogeneous nucleation and subsequent aggregation by Brownian motion. The plot of particle number concentration versus the sublimation temperature [Fig. 3(c)] shows the evaporation of large particles takes place at a temperature of 813 K. The evaporation temperature for large particles as obtained from Fig. 3(b) is indicated by an arrow for comparison implying an excellent agreement between the two experiments.

As discussed earlier, the agglomerates consist of small primary particles connected by sintering necks. Each primary particle has a convex surface and the sintering neck has a concave surface. Based on Kelvin equation, it can be shown that a convex surface produces a higher vapor pressure than does a planar surface and the reverse is the case for a concave surface. As the primary particles are small ($\sim$ 5.0 nm), the primary particles should evaporate at $\sim$577.4 K [estimated from Fig. 3(b)]. On the other hand, the size of the primary particles as well as the width of the sintering necks increases while increasing the sintering temperature. When the agglomerates are sintered at a moderate temperature, the increased solid-state diffusion coefficient allows one to form large primary particles with large sintering necks. However,

when the agglomerates are sintered at a high temperature, the vapor from the primary particles is believed to diffuse or condense on the necks of the agglomerates and they grow in size until the agglomerates are sintered completely to yield spherical particles. This means that there is no net evaporation from the agglomerates before complete sintering. This is supported by our optical absorption data as discussed in Ref. [7].

For a theoretical understanding of the observed size-dependent evaporation [Fig. 3(b)], we first examine the vapor pressure of small particles using the Kelvin equation. For the bulk vapor pressure (p_{s0}) of PbS, we use the expression

$$\log p_{s0}(\mathrm{Torr}) = -1.126 \times 10^4 \frac{1}{T(\mathrm{K})} + 5.809 \times 10^{-4} T(\mathrm{K}) + 9.3531, \quad (2)$$

which is obtained by fitting the data in the temperature range of 1028–1381 K [16]. As the evaporation of large particles is expected to take place at 805 K and the influence of the Kelvin effect can easily be neglected for large particles, the vapor pressure of PbS at this temperature is calculated to be 6.85×10^{-5} Torr. Using Eqs. (1) and (2), we estimate the temperature for different particle sizes to obtain the same vapor pressure as for large particles at 805 K, and the temperature is plotted against the inverse of the particle size as shown in Fig. 3(d) for different γ. A linear relationship is found between the temperature and the inverse of the particle size whose slope increases with the surface energy γ. Similar analyses for Au, Ag, and Si also show the linear relationship between the temperature and inverse of the particle size. Using γ as the free parameter to obey the Kelvin equation [Eq. (1)], a value of 2.45 $\mathrm{J/m^2}$ is obtained for PbS. As γ of PbS is not available for comparison, we use the empirical relation [17] to calculate γ when the bulk melting temperature of a solid is known. As the melting temperature of PbS is 1387 K, γ is calculated to be 1.4 $\mathrm{J/m^2}$, which is in reasonable agreement with that of an ionic semiconductor (~ 1 $\mathrm{J/m^2}$) but almost half of that deduced from Fig. 3(b). The large value of γ for PbS nanoparticles is consistent with the observations for CdS [9], Pt, and Au [18] and is attributed to a weak dilation of the surface of nanoparticles. It may also be noted that γ of free nanoparticles is higher as compared to the capped one [9] and, hence, a high value is expected for free PbS nanoparticles. In contrast, the free surface of the substrate-supported nanoparticles is almost half of their total surfaces and, hence, a smaller deviation from the reported value of γ has been obtained by Blackman *et al.* [4].

As evident from Fig. 3(d), the smaller particles evaporate at a certain temperature at which the large particles are still stable. This explains the mechanism of Ostwald ripening according to which large particles grow at the expense of smaller ones via evaporation, diffusion, and condensation. From the technological point of view, it is possible to evaporate different materials at the same temperature by taking different sized nanoparticles for different materials which may be useful for the synthesis of compound nanoparticles or thin films by evaporating different components from a single temperature source.

In summary, we have demonstrated that the size-dependent evaporation of free nanoparticles can be studied by the in-flight sintering technique. The variation of the evaporation temperature with particle size is found to be similar to the variation of the melting temperature and that both the entities depend on the surface energy of the material. This gives direct evidence of the Kelvin effect and allows one to estimate the surface energy of nanoparticles. The surface energy of PbS nanoparticles is found to be 2.45 $\mathrm{J/m^2}$, which is higher than for most ionic semiconductors and is attributed to the weak dilation of the surface.

We gratefully acknowledge Horst Zähres and S. Stappert for their help in TEM measurements. This work is financially supported by the Deutsche Forschungsgemeinschaft (DFG) in the framework of the special research programme "Nanoparticles from the gas-phase: formation, structure, properties" (SFB 445, project A7).

*Corresponding author.
Email address: nanda@uni-duisburg.de

[1] W. Thomson (Kelvin), Philos. Mag. **42**, 448 (1871).
[2] M. Schmidt *et al.*, Phys. Rev. Lett. **87**, 203402 (2001).
[3] M. Schmidt *et al.*, Nature (London) **393**, 238 (1998).
[4] M. Blackman, N. D. Lisgarten, and L. M. Skimmer, Nature (London) **217**, 1245 (1968).
[5] F. E. Kruis *et al.*, Appl. Phys. Lett. **73**, 547 (1998).
[6] F. E. Kruis, H. Fissan, and B. Rellinghaus, Mater. Sci. Eng. B **69-70**, 329 (2000).
[7] K. K. Nanda, F. E. Kruis, H. Fissan, and M. Acet, J. Appl. Phys. **91**, 2315 (2002).
[8] B. Rellinghaus, H. Mühlbauer, F. E. Kruis, H. Fissan, and E. F. Wassermann (unpublished).
[9] A. N. Goldstein, C. M. Echer, and A. P. Alivisatos, Science **256**, 1425 (1992).
[10] V. K. La Mer and R. Gruen, Trans. Faraday Soc. **48**, 410 (1952).
[11] L. R. Fisher and J. N. Israelachvili, Nature (London) **277**, 549 (1979).
[12] L. R. Fisher, R. A. Gamble, and J. Middlehurst, Nature (London) **290**, 575 (1981).
[13] W. C. Hinds, *Aerosol Technology* (Wiley, New York, 1982), p. 44.
[14] H. Dixkens and H. Fissan, Aerosol Sci. Technol. **30**, 438 (1999).
[15] D. H. Lowndes *et al.*, J. Mater. Res. **14**, 359 (1999).
[16] L. Gmelin, in *Gmelin Handbook of Inorganic Chemistry*, edited by E. H. E. Pietsch (Springer, Berlin, 1979).
[17] K. K. Nanda, S. N. Sahu, and S. N. Behera, Phys. Rev. A **66**, 013208 (2002).
[18] C. Solliard and M. Flueli, Surf. Sci. **156**, 487 (1985).